

Fast deformation of perennially frozen debris in a warm rock glacier in the Swiss Alps: An effect of liquid water

Atsushi Ikeda,¹ Norikazu Matsuoka,¹ and Andreas Kääb²

Received 30 June 2007; revised 25 October 2007; accepted 18 December 2007; published 21 March 2008.

[1] Surface movement, internal deformation, and temperature were monitored over 5 years on Büz North rock glacier, a small rock glacier located at the lower limit of the permafrost belt in the Swiss Alps. The permafrost in the rock glacier mainly consists of pebbles and cobbles filled with interstitial ice. Two inclinometers installed at 4 and 5 m depths showed fast deformation with large seasonal and interannual variations, while the permafrost temperatures remained almost at the melting point. The movement of the inclinometers coincided with changes in the surface velocities. The deformation rapidly accelerated during snowmelt periods, whereas it gradually decelerated below a dry snow cover in winter. The frozen debris was more deformable than typical glacier ice at the melting point. These phenomena suggest that the frozen debris is permeable to snowmelt water. The fast deformation should result from significant annual relocation of debris particles, which probably creates a network of air voids in the frozen debris that eventually allows water infiltration. The meltwater infiltration accelerates the deformation by reducing effective stress, resulting in the reduced strength of the frozen debris. The refreezing of the pore water, which depends on the cooling intensity in winter, decelerates the deformation. The combination of these processes controls the temporal variations in the deformation.

Citation: Ikeda, A., N. Matsuoka, and A. Kääb (2008), Fast deformation of perennially frozen debris in a warm rock glacier in the Swiss Alps: An effect of liquid water, *J. Geophys. Res.*, 113, F01021, doi:10.1029/2007JF000859.

1. Introduction

[2] Surface velocities of rock glaciers determined by geodetic survey, aerial photogrammetry, or radar interferometry are typically a few centimeters to a few meters per year [e.g., *Wahrhaftig and Cox*, 1959; *Haeberli et al.*, 1979; *Kääb et al.*, 1997, 2002, 2003; *Strozzi et al.*, 2004], which are orders of magnitude lower than typical velocities of temperate alpine glaciers [cf., *Raymond*, 1980]. On the basis of direct measurements with slope inclinometers installed in boreholes, the slow movements of rock glaciers have been attributed to gravity-driven continuous deformation of perennially frozen debris a few tens of meters thick [*Johnson and Nickling*, 1979; *Wagner*, 1992; *Hoelzle et al.*, 1998; *Arenson et al.*, 2002]. The slow velocities also imply that many rock glaciers have developed by continuous “permafrost creep” over several thousands of years [*Haeberli*, 1985, 2000; *Frauenfelder et al.*, 2005; *Haeberli et al.*, 2006]. For example, the ¹⁴C ages (mean 2250 years B.P.) of moss remains obtained from a borehole on Murtèl rock glacier, Swiss Alps, and isochrones extrapolated from the present-day surface velocity fields indicate that the rock glacier has continuously developed over at least 5000 years

and probably the entire Holocene [*Haeberli et al.*, 1999]. In this steady (i.e., slow, continuous movement) model, long-term climatic warming inactivates rock glaciers through melting of ice [*Barsch*, 1992; *Ikeda and Matsuoka*, 2002].

[3] Whereas the steady model has been applied to the development of many rock glaciers, relatively fast and variable movements have recently been addressed under ongoing warming trends. High surface velocities (>0.2 m a⁻¹) were observed on the rock glaciers whose front had reached the lower limit of local permafrost occurrence [*Frauenfelder and Kääb*, 2000; *Frauenfelder et al.*, 2003; *Kääb et al.*, 2007]. A positive correlation has been found between the permafrost temperature and mean annual or seasonal surface velocity on rock glaciers [*Hoelzle et al.*, 1998; *Arenson et al.*, 2002; *Kääb et al.*, 2003]. Simultaneous acceleration of many rock glaciers in a mountain range appears to follow regional climatic warming trends [*Roer et al.*, 2005]. These findings indicate that the atmospheric and subsequent ground warming accelerates rock glaciers [*Kääb et al.*, 2007], because frozen soils become more deformable as temperature rises toward their melting point [e.g., *McRoberts et al.*, 1978; *Morgenstern et al.*, 1980]. Rheological tests of ice with various debris contents also suggest that rock glacier permafrost generally becomes more rigid with decreasing “ice supersaturation” (i.e., ice volume exceeding the pore volume) because of the increasing friction between soil particles [*Nickling and Bennett*, 1984; *Arenson and Springman*, 2005a, 2005b]. In situ subsurface deformation of ice-debris mixtures verifying the laboratory

¹Graduate School of Life and Environmental Sciences, University of Tsukuba, Tsukuba, Japan.

²Department of Geosciences, University of Oslo, Oslo, Norway.

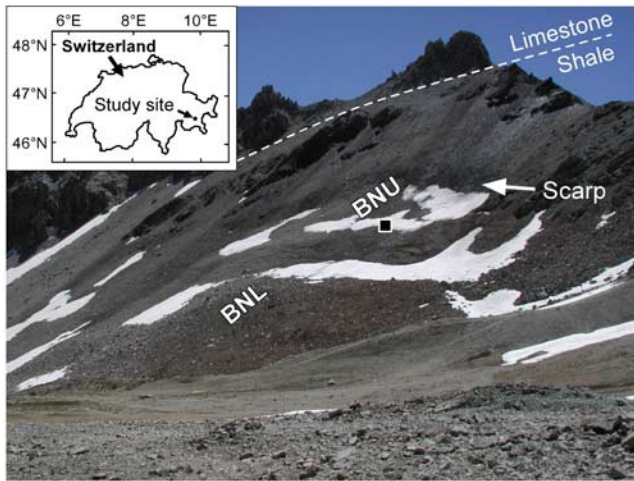


Figure 1. Büz North (BN) rock glacier consists of the upper lobe (BNU) and the lower lobe (BNL). The position of the borehole is indicated by the square. Location of the rock glacier in Switzerland in the inset.

findings was, however, rarely observed in spite of a number of studies on rock glacier dynamics. In addition, the influence of liquid water on mobilizing rock glaciers remains unsolved [Arenson and Springman, 2005b]. Thus, this study focuses on the in situ deformation of a warm ice-debris mixture in a rock glacier.

[4] To overcome the problem that the bouldery internal structure of many rock glaciers complicates drilling, we investigated a thin “pebbly” rock glacier [Ikeda and Matsuoka, 2006] covered with pebbles and cobbles (2–15 cm in intermediate axis diameter), in which perennially frozen debris appeared to be deformed largely at shallow depth [Ikeda et al., 2003]. The rock glacier is located at the lower limit of the permafrost belt in the Upper Engadin,

eastern Swiss Alps. We performed annual geodetic surveys and continuous monitoring of internal deformation and ground temperature. On the basis of the observed movements and ground thermal conditions, we discuss the dynamics of this small, warm ($\sim 0^\circ\text{C}$ in the permafrost), active rock glacier, potentially vulnerable to environmental change. In particular, this monitoring implies the complex nature of frozen soil with abundant pebbles, cobbles, and liquid pore water. The rock glacier under study is talus-derived and too small to apply glacier-like development models, which have been used for large rock glaciers [e.g., Whalley and Martin, 1992; Humlum, 1996; Potter et al., 1998].

2. Study Site

[5] The studied rock glacier is Büz North (BN) rock glacier (latitude: $46^\circ 32' \text{N}$, longitude: $9^\circ 49' \text{E}$), located on the northeastern slope of a peak named Piz dal Büz (2955 m above sea level), which is composed of shale bedrock overlain by a limestone caprock (Figure 1, see also Ikeda and Matsuoka [2006] for the details of the location). BN rock glacier originates from the foot of a talus slope at 2840 m above sea level (asl) and terminates at 2775 m asl. BN consists of the upper lobe (BNU), 70 m long and 120 m wide, and the lower lobe (BNL), 90 m long and 100 m wide (Figures 1 and 2). BNU has a steep front 10 m high, sloping at 35° , while BNL lacks a distinct front. The upper surface is smooth and the average slope angles are 25° on BNU, 15° on the upper part of BNL, and 25° on the lower part of BNL. The ground surface consists mainly of shale pebbles and cobbles and lacks vegetation cover. Limestone boulders are scattered on the surface.

[6] The talus slope above the rock glacier is 40–50 m high, of which the upper part slopes at $35\text{--}40^\circ$ and the lower part at $40\text{--}45^\circ$ (Figure 2). The steep lower part resembles a landslide scarp, and unstable debris below the talus slope indicates active slip processes. In fact, the

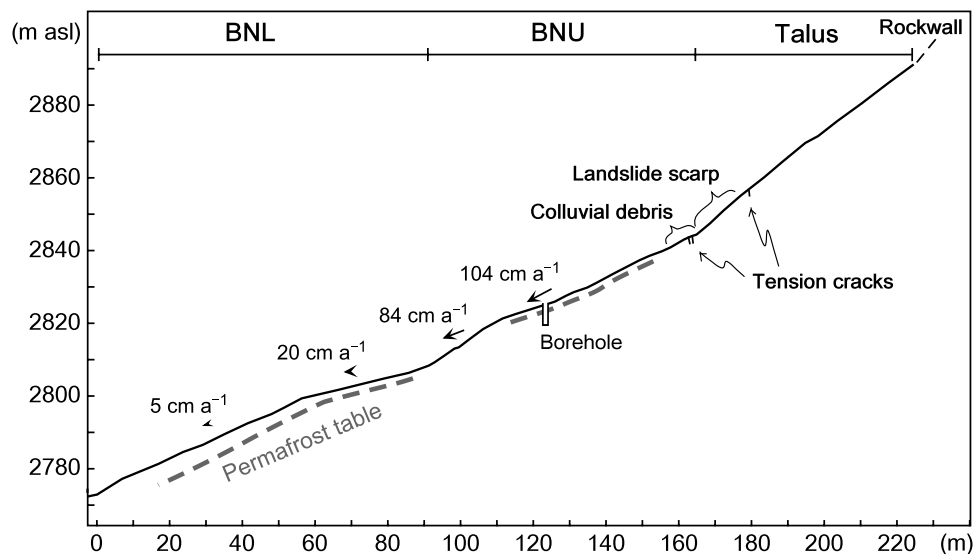


Figure 2. Surveyed longitudinal profile of BN rock glacier. The steep lower part of the talus slope results from recent erosion accompanying the downslope movement of BNU. The vectors indicate the average surface velocities for 1998–2005 at the upper surface of BNU, frontal slope of BNU, upper part of BNL, and lower part of BNL. The length of the vectors on BNU represents the total displacement for 7 years. The depth of the permafrost table was estimated by seismic soundings.

unstable scarp has gradually enlarged by small landslides, debris flows, and rockfalls during the observed period. Several tension cracks parallel to the scarp face developed behind the scarp and on the upper part of the landslide deposit in 2002.

[7] A pit and borehole dug on BNU in early August 2000 indicated that the major components are platy shale pebbles and cobbles whose interstices are partly filled with sand and silt [Ikeda and Matsuoka, 2006]. Below the frost table (1 m deep on 3 August 2000), the debris was entirely ice cemented to the bottom of the hole (5.4 m deep) and lacked visible air voids. Thin ice veins (<2 cm thick) nearly parallel to the surface were observed below 2 m depth. The gravimetric ice content of borehole cores (~10 cm long) was 50% at 4 m depth and 28% at 5 m depth. On the assumption of no air voids, the volumetric ice content was computed to be about 60% at 4 m depth and 45% at 5 m depth. The borehole did not reach the bedrock at the bottom.

[8] Seismic refraction soundings revealed a two-layered structure in the rock glacier [Ikeda, 2006]. The seismic refraction of BNU and the upper part of BNL showed unfrozen surface layers mostly shallower than 3 m, whereas that of the lower part of BNL showed an unfrozen top layer 4 to 6 m thick, implying permafrost has been degraded near the terminus of the rock glacier (Figure 2). One-dimensional and two-dimensional DC resistivity measurements showed that the resistivity values in BN are of the order of 1 k Ω m [Ikeda and Matsuoka, 2006], which is the lowest range for a frozen core in active and inactive rock glaciers [Haeberli and Vonder Mühll, 1996; Ikeda, 2006]. Such low values probably result from the debris-rich frozen layer at temperatures close to the melting point. Massive ice, which generally has a high DC resistivity (>100 k Ω m), is unlikely to exist in the rock glacier.

3. Methods

[9] The surface displacements of the BN rock glacier were measured annually from August 1998 to July 2005 by combined triangulation and laser ranging survey of marker boulders. Two benchmarks were placed on limestone outcrops around the rock glacier by anchoring a steel bolt. Five survey points were constructed on BNU and 8 points on BNL. The three-dimensional angles and distances from the two benchmarks to all markers on BN were measured using a total station Leica TCA 1102. The accuracy of the millimeter scale was guaranteed by inserting the tapered tip of a reflector in an 8 mm diameter drill hole on the marker boulders. The total error produced by the survey system was less than 1 cm a⁻¹. The benchmarks and survey points were established on 11 August 1998. These points were annually resurveyed on 22 July 1999, 24 July 2000, 2 August 2001, 19 July 2002, 13 August 2003, 4 October 2004, and 27 July 2005.

[10] The internal movement of BNU was measured with inclinometers from 9 August 2000, when the third year of the survey started, to 24 July 2005. Two inclinometers (BKJ-A-10-D, manufactured by Kyowa Electronic Instruments, Japan), 35 cm long and 2.7 cm in diameter, were installed at 4 and 5 m depths in the borehole (see Figure 1 for the location). The inclinometers sensed inclinations along two directions perpendicular to each other. The

inclinometers can measure inclinations within $\pm 12.2^\circ$ from the vertical, with a resolution of 0.005° . The inclinations were recorded by a data logger (EXL-007A-8, LOG Electronics, Japan) at 3 h intervals until July 2003 and 6 h intervals thereafter.

[11] The inclination at a certain depth was calculated from the sum of the horizontal vectors, which were defined as the tangents of the measured inclinations for the two axes. The inclinations were used to calculate a creep parameter in a simple flow law for ice and frozen soil in a vertical plane:

$$\dot{\epsilon} = dv/dz = 2A\tau^n, \quad (1)$$

where $\dot{\epsilon}$ is the downslope (i.e., direction parallel to surface dip) strain rate, v is the downslope velocity at a depth, z is the depth perpendicular to the surface, τ is the downslope shear stress, A is a constant for a given temperature and structure, and n is an experimentally derived exponent [e.g., Glen, 1955; Morgenstern et al., 1980; Paterson, 1994]. The strain rate $\dot{\epsilon}$ equals the vertical velocity gradient dv/dz . The exponent $n \approx 3$ is most often used in the flow law of ice and ice-rich silty soil [e.g., Morgenstern et al., 1980; Hooke, 1981], whereas n is close to 2 for frozen coarse debris with 50–70% ice content [Arenson and Springman, 2005b]. In addition, high temperatures ($> -1^\circ\text{C}$) and/or low shear stresses (<50 kPa) possibly result in n close to 2 or smaller [Mellor and Testa, 1969a, 1969b; Morgenstern et al., 1980; Wang and French, 1995]. The shear stress at a depth z is:

$$\tau = \rho g |z| \sin \alpha, \quad (2)$$

where ρ is the mean density of rock glacier components, g is the acceleration due to gravity (9.8 m s^{-2}), $|z|$ is the absolute value of z , and α is the surface gradient. The creep parameter A was calculated for the two depths using $\rho = 1800 \text{ kg m}^{-3}$ and $\alpha = 25^\circ$ (average angle of the whole upper surface) and for n fixed to 1, 2, and 3.

[12] Ground surface temperature was monitored with two miniature data loggers (Thermo Recorder TR-51A, T & D, Japan) placed on BNL on 6 August 1998, and on BNU on 11 August 1999. The loggers recorded temperatures under a 3–4 cm thick clast at 1 h intervals with a resolution of 0.1°C . From the third year, six thermistor probes were installed at depths of 0.5, 1, 2, 3, 4, and 5 m in the borehole. These data have been recorded in a data logger (KADEC-UN, Kona System, Japan) at 1 h intervals with a resolution of 0.1°C from 9 August 2000 to 22 July 2005. The recorded ground temperatures were calibrated by fitting the persistently constant temperature near the melting point (the zero curtain) into 0.0°C ; hence, the error near 0°C was $\pm 0.1^\circ\text{C}$. In addition, the thickness of the snow cover was manually measured on 3 March 1999, 22 March 2001, and 6 March 2002 to evaluate the interannual variations of snow conditions (thickness, duration, timing of snowfall) that control ground temperature [e.g., Vonder Mühll et al., 1998; Hoelzle et al., 2003].

4. Surface Movements and Variables

4.1. Surface Velocity

[13] Surface movement of BN rock glacier showed large spatial and temporal variations (Table 1, Figure 3). The

Table 1. Annual Surface Velocities and the Dips of the Velocities to the Horizontal Plane^a

| Period | Büz North Upper Lobe | | | | Büz North Lower Lobe | | | |
|----------------------------|----------------------------|--------------|----------------------------|--------------|----------------------------|----------------|----------------------------|--------------|
| | Upper Surface | | Frontal Slope | | Upper Part | | Lower Part | |
| | V_S (m a ⁻¹) | θ (°) | V_S (m a ⁻¹) | θ (°) | V_S (m a ⁻¹) | θ (°) | V_S (m a ⁻¹) | θ (°) |
| 11 Aug 1998 to 22 Jul 1999 | 0.74–0.82 | 26 | 0.49–0.58 | 19 | 0.08–0.19 | 17 | 0.02–0.06 | 13 |
| 22 Jul 1999 to 24 Jul 2000 | 0.84–0.95 | 29 | 0.66–0.73 | 21 | 0.10–0.23 | 2 ^b | 0.02–0.06 | 24 |
| 24 Jul 2000 to 2 Aug 2001 | 1.34–1.46 | 27 | 1.09–1.14 | 19 | 0.16–0.37 | 7 | 0.04–0.09 | 11 |
| 2 Aug 2001 to 19 Jul 2002 | 0.88–0.96 | 28 | 0.78–0.79 | 21 | 0.15–0.33 | 2 ^b | 0.03–0.08 | 14 |
| 19 Jul 2002 to 13 Aug 2003 | 0.95–1.04 | 28 | 0.83–0.85 | 21 | 0.18–0.36 | 1 | 0.03–0.07 | 10 |
| 13 Aug 2003 to 4 Oct 2004 | 1.16–1.24 | 29 | 1.02–1.04 | 22 | 0.17–0.43 | 8 | 0.03–0.10 | 20 |
| 4 Oct 2004 to 27 Jul 2005 | 0.94–1.03 | 28 | 0.82–0.86 | 22 | 0.19–0.42 | 0 | 0.04–0.11 | 8 |
| 11 Aug 1998 to 27 Jul 2005 | 0.98–1.07 | 28 | 0.83–0.85 | 21 | 0.15–0.33 | 4 | 0.02–0.08 | 15 |

^a V_S , annual surface velocities; θ , angles of depression.^bAngles of elevation.

marker boulders on BNU moved much faster than those on BNL in every year. The average downslope velocities V_S for the 7 years were 98–107 cm a⁻¹ at the three points (11–13) on the upper surface of BNU, 83–85 cm a⁻¹ at the two points (9–10) on the frontal slope of BNU, 15–33 cm a⁻¹ at the five points (4–8) on the upper part of BNL, and 2–8 cm a⁻¹ at the three points (1–3) on the lower part of BNL. Thus, the frontal slope of BNU moved about 0.8 times as fast as the upper surface and the velocities on BNL also decreased from the upper part to the lower part. Late-lying snow cover often prevented remeasurement of point 7, so that the annual velocities of the marker are not included in Table 1 and Figure 3.

[14] All points moved horizontally in consistent directions over the 7 years (Figure 3). The dips of the velocities to the horizontal plane (θ) were also constant on BNU, while those on BNL showed large annual variations (Table 1). The marker boulders on BNU moved nearly parallel to the upper surface (25°), which indicated the advance of the steep frontal slope with a gradient of 35° [see also Kääb *et al.*, 2007, Figure 7]. The boulders on BNL moved upward to the surface. In particular, significant uplift of the upper part of BNL is indicated by the large difference between θ (on average, 4° for 7 years) and the local slope gradient (17°), which probably reflected the compressive stress field between the fast moving BNU and the slowly moving lower part of BNL.

[15] Downslope movement of BN slightly accelerated from the first year (1998–1999) to the second year (1999–2000), on average, by 20% (Figure 4a). In the third year (2000–2001), the V_S values significantly increased to twice those of the first year. In the fourth year (2001–2002), BNU decelerated, while BNL maintained the velocities. As a result, the velocities of BNU and BNL in the fourth year were 1.3 times and 1.7 times larger than those in the first year, respectively. Movement of BNU gradually accelerated again from the fourth to the sixth year (2003–2004) and decelerated to the seventh year (2004–2005). The velocities of BNU in the fifth, sixth, and seventh years were 1.4 times, 1.7 times, and 1.4 times as large as those in the first year, respectively. In contrast to BNU, BNL showed nearly constant or slightly increasing velocities after the fourth year.

[16] Downslope soil movement within the active layer was very small. Flexible probes installed perpendicular to the surface showed that the surface movement within the

active layer amounted only to 0.8 to 1.6 cm a⁻¹ downslope on BNU over 3 years (2000–2003) and 0.4 cm a⁻¹ downslope on the upper part of BNL over 5 years (1998–2003) (Figure 5). The velocity profiles are typical of

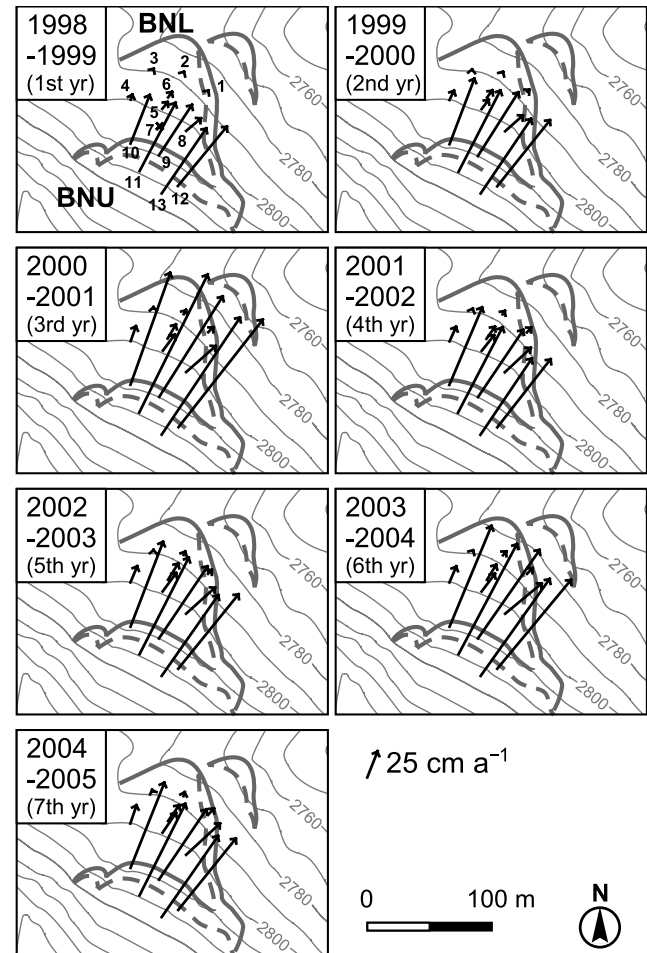


Figure 3. Annual horizontal displacements of marker boulders over 7 years. The cardinal and ordinal numbers in the top left in each box indicate the periods of the observation. The point numbers of the marker boulders are also shown in the first box. The solid lines indicate the lower margin of a lobe, and the dashed lines indicate the upper edge. Contour interval 10 m.

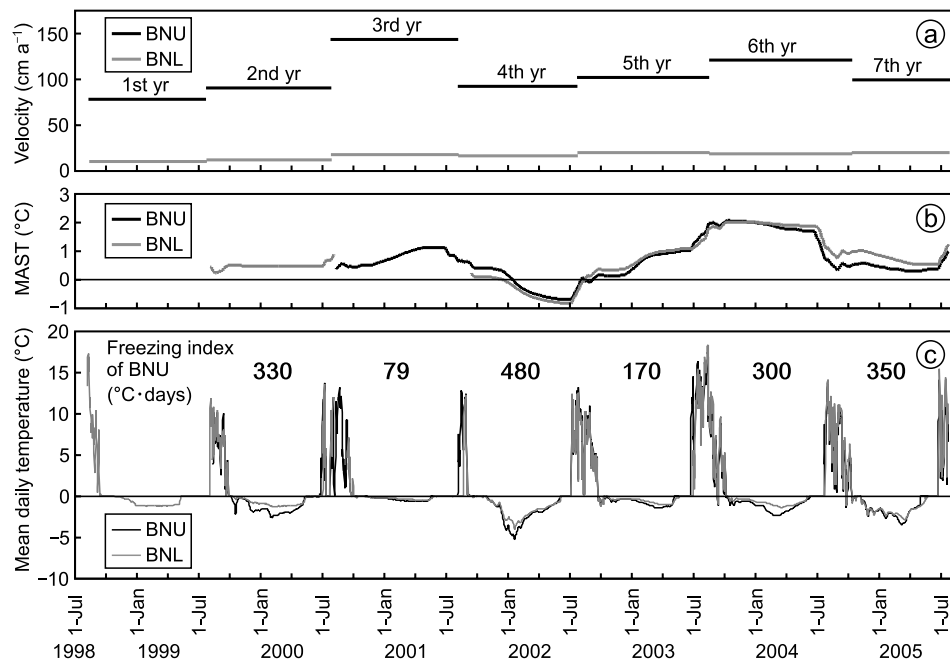


Figure 4. The 7 year record of (a) annual surface velocity, (b) running mean of annual surface temperature (MAST), and (c) daily mean of ground surface temperature on BNU and the upper part of BNL. The temperature records on BNU started on 11 August 1999, and those on BNL were interrupted from 3 August to 11 September 2000.

solifluction [cf., Matsuoka, 2001]. The small velocities of the solifluction on the relatively steep slope [cf., Matsuoka *et al.*, 1997] probably reflected the low content of frost susceptible fine debris. The movements of the marker boulders were unlikely to result from active layer slides or debris flow, because the boulders lacked any trace of such a rapid displacement during the observation period. Consequently, the major part of the boulder movements was attributed to deformation within the permafrost.

4.2. Snow Thickness

[17] During the observed period, the thickness of the snow cover fluctuated year by year. On 3 March 1999 (first year), the snow depth ranged from 1.5 to 2.8 m (average 2.3 m) among 8 points on BN. On 22 March 2001 (third year), the snow depth exceeded 4 m on BNU and 5 m on the upper part of BNL. On 6 March 2002 (fourth year), the snow depth on BN ranged from 0.8 to 2.4 m among 11 points (average 1.6 m). The annual variations in ground surface temperatures observed around BN in the first and second years [Ikeda and Matsuoka, 2002] were typical of those in the Upper Engadin [Vonder Mühll *et al.*, 1998]. In such a case, the ground is cooled under thin snow cover in early winter and then thickening dry snow cover (>0.8 m deep) in late winter insulates the ground from the air temperature [Hoelzle *et al.*, 1999]. In contrast to the first and second year, the thick snow in the third year and the thin snow in the fourth year reflected abnormal conditions: sudden and heavy snowfalls in October and November 2000 prevented the ground from cooling; and lack of notable snowfalls until late January 2002 resulted in intensive ground cooling [Hoelzle *et al.*, 2003].

4.3. Surface Temperature

[18] Continuous subzero cold season temperatures at the surface of BN indicate that BN was covered with snow for more than 9 months per year (Figure 4c). In the first and second years with normal snow conditions, the temperature on BNL gradually decreased in early winter, and remained nearly constant at about -1°C until mid-May, when the temperature rapidly rose to 0°C as a result of snowmelt. The winter temperature on BNU in the second year decreased stepwise to -2.5°C , and gradually increased until mid-May. The winter temperatures in the sixth year (2003–2004) showed similar variations. The extremely thick snow cover in the third year kept surface temperatures at -0.5°C during the whole winter on both BNU and BNL. The snow remained until early August on BNU and late August on BNL, which means that the meltout of the snow cover

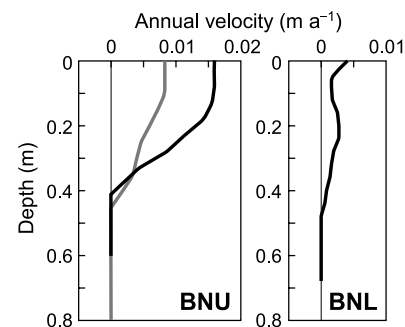


Figure 5. Deformation profiles in the active layer, indicated by flexible probes. The profiles of two probes installed near the borehole on BNU are indicated by different colors.

lagged one month behind that in the normal years. In contrast, the thin snow cover in the fourth winter resulted in relatively unstable temperatures falling to -5°C on BNU and -4°C on BNL. The temperatures in the fifth winter suggested that the snow condition was intermediate between the normal winters and the snow-rich third winter. In the seventh winter, the relatively unstable temperatures reaching about -3°C indicated that the snow cover was thin compared with the normal winters. Freezing indices also demonstrated a large interannual variation of ground cooling in winter ($79\text{--}480^{\circ}\text{C days}$) (Figure 4c).

[19] Figure 4b indicates the temporal variation in mean annual ground surface temperature (MAST), which was averaged for the preceding 365 days (i.e., running means of the temperatures in Figure 4c). The available data showed nearly the same variations in MASTs on BNU and BNL, which ranged from -0.8 to 2.0°C . The MASTs, which were mostly above 0°C (except in 2002), indicated recent warming of the permafrost in this rock glacier because the ground surface lacks any buffering layer such as matrix-free boulders or a thick organic mat.

[20] MASTs were nearly constant in the second year. MAST on BNU was 0.4°C at the beginning of the third year (August 2000) and gradually increased to 1°C until May 2001. Such a rise in MAST resulted mainly from the high winter temperature despite the long lasting snow cover preventing the ground from warming. The intensive ground cooling in 2001–2002 resulted in the minimum MASTs (-0.7°C on BNU and -0.8°C on BNL). Through the following 2002 summer and 2002–2003 winter with thick snow cover, MASTs rose to 1°C until the end of March 2003, which was similar to the value in the 2001 spring. The highest MASTs (2.0°C) were reached in the late summer of 2003, which reflected the extremely hot summer. The high temperatures melted the snow before the end of June, despite the presence of thick snow in the preceding winter. During the following normal summer (2004), MASTs decreased to the values similar to those in August 2000.

[21] MASTs showed similar interannual variations to the surface velocities on BNU (Figure 4). However, the highest velocity (2000–2001) did not correspond to the highest MASTs (2003–2004) but to the smallest freezing index.

5. Subsurface Movements and Variables

5.1. Strain Rate of the Perennially Frozen Debris

[22] The two inclinometers installed in BNU rock glacier showed large tilting in the perennially frozen debris, which corresponded to the high surface velocity (Figures 6a and 6b). Both continuously moved over the observation period (2000–2005). The directions of inclinations were consistent during the 5 years, except for the first two days after the installation, during which the dissipation of the thermal disturbance from the drilling procedure took place and materials around the inclinometers were probably refreezing. The inclination at 5 m depth always exceeded that at 4 m depth, and inclination for one of the two axes at 5 m depth exceeded the measurement limit on 3 February 2003. Thereafter, the inclination at 5 m depth was estimated from the measured inclination for the other axis using the linear relationship between inclinations for the two axes ($r^2 =$

0.9995) before 3 February 2003. The average tilting rates at 4 and 5 m depths in the observed period were $2.5^{\circ} \text{ a}^{-1}$ and $6.0^{\circ} \text{ a}^{-1}$, respectively.

[23] The strain rates calculated from the inclinations displayed both seasonal and interannual variations (Figure 6c). The weekly strain rates ranged from 0.00 to 0.09 a^{-1} at 4 m depth and from 0.01 to 0.27 a^{-1} at 5 m depth. The annual strain rates at 5 m depth, determined from the increments between the days of the annual triangulation surveys, were calculated to be 0.18 a^{-1} , 0.093 a^{-1} , 0.11 a^{-1} , 0.13 a^{-1} , and 0.12 a^{-1} in chronological order from 2000–2001 to 2004–2005 (i.e., from the third year to the seventh year of the surface measurements). The annual strain rates at 4 m depth were about one third of the rates at 5 m depth. These interannual variations paralleled the variation in surface velocities (see Figure 6a).

[24] The pattern of the seasonal variations was also parallel between the two depths. Strain rates rapidly increased when the whole snow cover became wet (May to early June), as indicated by the sudden rise in ground surface temperature to the melting point (Figures 6d and 7). The strain rates began to decrease in the middle of the snowmelt period (June to early July) and became almost constant in midsummer (July to early August), when the snow disappeared at the monitoring site or had disappeared one to two weeks before. There was usually a net increase in strain rates during the snowmelt period. After the summer decrease, the strain rates slightly increased or remained constant for several months before starting to decrease in the following winter. The magnitudes of the winter decrease in strain rates appear to have depended on the cooling intensity of the ground surface. In the warmest winter (2000–2001), the strain rates were stable. In the winters of 2002–2003, 2003–2004, and 2004–2005, the decrease in strain rate at 4 m depth started one to two months earlier than that at 5 m depth.

5.2. Creep Parameter of the Perennially Frozen Debris

[25] Using equations (1) and (2), creep parameters A_4 at 4 m depth ($|z| = 3.8 \text{ m}$) and A_5 at 5 m depth ($|z| = 4.7 \text{ m}$) were calculated for each year (Table 2). In addition, a creep parameter A_{4-5} over 4–5 m depth ($|z| = 3.8\text{--}4.7 \text{ m}$) was calculated using the average of the measured strain rates for each year. Note that $|z|$ is the absolute value of a depth perpendicular to the surface. A_5 was 1.5–2.5 times greater than A_4 , which indicates more deformable structure at 5 m depth. Smaller n values resulted in larger differences in A between the two depths (Table 2). The maximum A_5 values derived from the maximum weekly strain rate at 5 m depth in 2001 were $1.5 \times 10^{-10} \text{ kPa}^{-1} \text{ s}^{-1}$ ($n = 1$), $4.4 \times 10^{-12} \text{ kPa}^{-2} \text{ s}^{-1}$ ($n = 2$), and $1.3 \times 10^{-13} \text{ kPa}^{-3} \text{ s}^{-1}$ ($n = 3$), which were twice the mean annual values for 2000–2001.

[26] The next step is to estimate the thickness of the moving debris H perpendicular to the surface. From equations (1) and (2), we obtain

$$V_S = 2A(\rho g \sin \alpha)^n \int_0^H |z|^n dz. \quad (3)$$

Assuming that A_{4-5} is representative for the whole frozen layer, neglecting small deformation ($<2 \text{ cm a}^{-1}$) of the

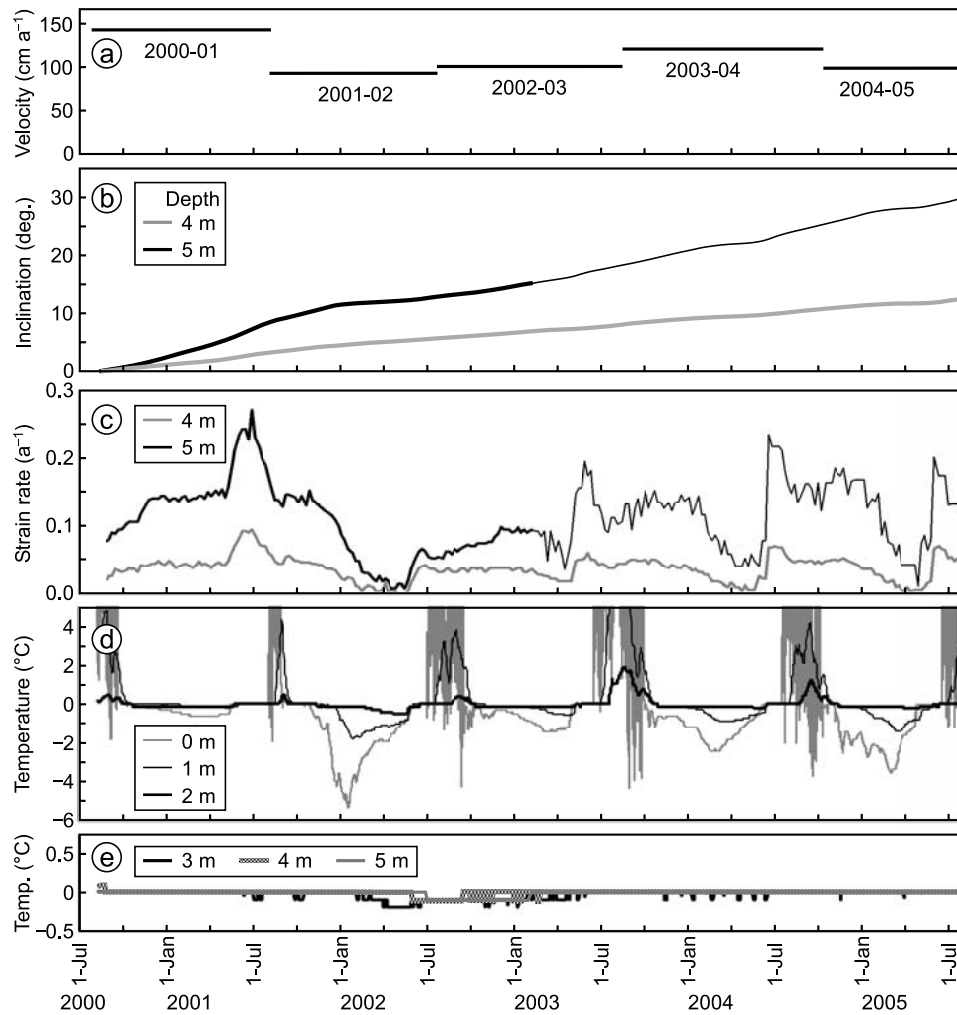


Figure 6. The 5 year record of (a) surface velocity, (b) inclination, (c) strain rate, (d) active layer temperature, and (e) permafrost temperature of BNU. The thin lines in Figure 6b and 6c indicate that only one of the two axes sensed the inclination.

active layer (in the uppermost 2 m) and using the observed average V_S values for each year, extrapolation shows that the vertical height of deformed sediment H_V was about 9 m thick ($H \approx 8$ m) for $n = 3$ and about 10 m thick ($H \approx 9$ m) for $n = 2$ (Table 2, Figure 8). The H_V values for each n value were roughly consistent in the 5 years and those for $n = 2$ to 3 approximated the frontal height (~ 10 m) of BNU. In contrast, the H_V values for $n = 1$ (11–12.5 m) exceeded the thickness of the rock glacier (Table 2). Since deformation in a rock glacier generally occurs within the thickness indicated by the frontal height [Kääb and Reichmuth, 2005], the n values between two and three are appropriate to depict the vertical velocity profiles from the obtained data, although the calculation indicates that 80–90% of the surface velocity originates from deformation below the inclinometers (Figure 8), where A and n values may differ from the applied values.

5.3. Ground Temperature

[27] Permafrost temperatures (at 3–5 m depth) were nearly constant at 0.0°C through the 5 years (Figure 6e). Temperatures at 4 and 5 m depths decreased to -0.1°C only after the winter with the shallow snow (i.e., the latter half of

2002). The temperatures at 3 m depth reached -0.2°C in the same winter and remained at -0.1°C until the end of the following winter.

[28] The maximum thickness of the active layer was about 2.2 m in 2000, 2001, 2002, whereas it probably reached 2.5 m in the extremely hot summer of 2003. The moderately warm summer of 2004 also resulted in deep seasonal thawing (~ 2.4 m). The temperatures at 1 to 3 m depth remained at -0.1 to 0.0°C throughout the winter of 2000–2001 because of the extremely thick snow cover (Figure 6c–6d). In contrast, temperatures in the uppermost 2 m dropped to -3.0°C , -1.8°C , and -0.5°C at 0.5, 1, and 2 m depths, respectively, under the shallow snow in the winter of 2001–2002. In the following winters, temperatures were between those in the two extreme winters.

6. Factors Affecting Deformation of Ice-Debris Mixture

6.1. Softness of the Perennially Frozen Debris

[29] Both triangulation and inclinometer measurements showed large deformation of the perennially frozen debris in BNU rock glacier. An analysis based on the observed

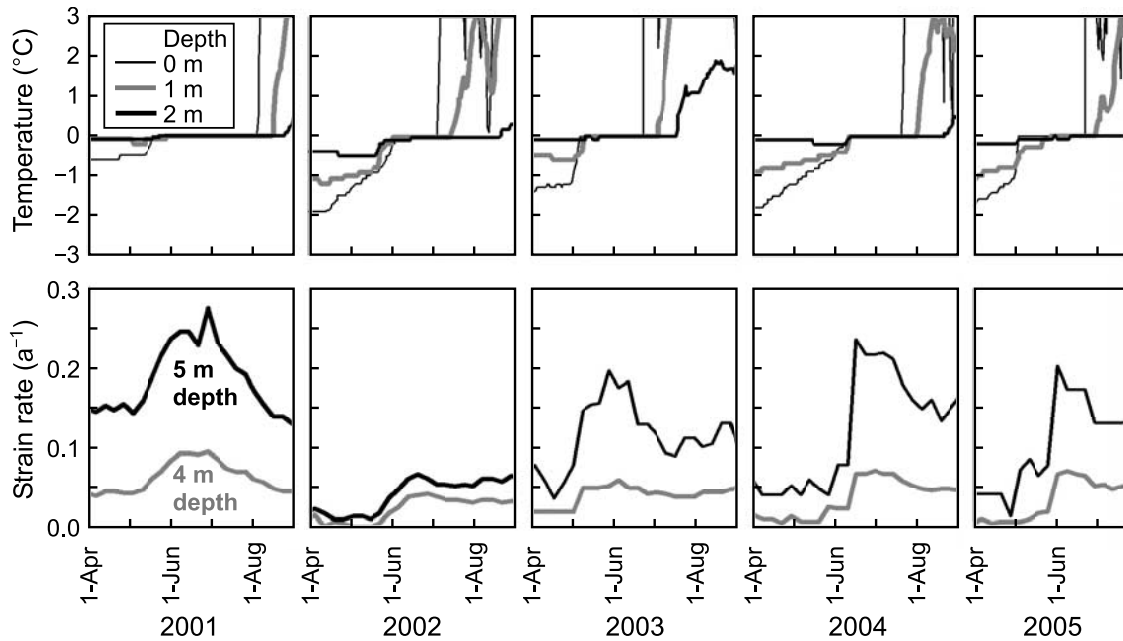


Figure 7. (top) Daily mean temperatures in the active layer in the snowmelt periods of 2000–2005. (bottom) Strain rates in the permafrost in the same periods. Note that the temperatures in the permafrost (3, 4, and 5 m depths) during these periods were nearly constant at the melting point (-0.2 – 0.0°C).

inclinations and a flow law indicated that the deformation of BNU occurred within the top 10 m. The large deformation primarily reflected the steep slope ($\sim 25^{\circ}$) and the permafrost temperature at the melting point.

[30] The calculated creep parameter A for frozen pebbles and cobbles of BNU is higher than the previously reported values for polycrystalline ice. For the exponent $n = 3$, the annual A_5 values of BNU (see Table 2) are more than five times higher than a well-cited value for glacier ice at 0°C ($6.8 \times 10^{-15} \text{ kPa}^{-3} \text{ s}^{-1}$) [Paterson, 1994, p. 97]. Laboratory data compiled by Budd and Jacka [1989] indicated a slightly higher A value for polycrystalline ice at 0°C ($9.3 \times 10^{-15} \text{ kPa}^{-3} \text{ s}^{-1}$), but the value is still lower than those of BNU. The parameter A for in situ deformation of glacier ice would be even lower than the Paterson's value [e.g., Hubbard et al., 1998; Gudmundsson, 1999]. The A values for ice-supersaturated fine soil under steady state creep hardly exceed those of polycrystalline ice [e.g., McRoberts et al., 1978; Savigny and Morgenstern, 1986]. In addition, an increase in debris content strengthens the frozen soil owing to interlocking of soil particles larger than sand size [e.g., Hooke et al., 1972; Nickling and Bennett, 1984].

These results contradict the softness of the ice-debris mixture in BNU.

[31] In contrast to the strength of polycrystalline ice and frozen soils derived from laboratory tests, the huge Fireweed rock glacier in Alaska had surface velocity fields requiring A values at least twice those of clean temperate ice [Bucki and Echelmeyer, 2004]. The high A values indicating soft frozen ground appear to be associated with the large amount of debris, which was in fact seen at the calved front [Elconin and LaChapelle, 1997; Bucki et al., 2004]. Bucki and Echelmeyer [2004] considered that the large A values originated from interstitial water between debris particles and ice crystals, which possibly allowed slip at the interface by lowering the effective viscosity, as Echelmeyer and Wang [1987] and Cohen [2000] explained the softness of dirty basal ice. Cohen [2000] proposed quite large A values (1.4×10^{-14} – $1.4 \times 10^{-13} \text{ kPa}^{-3} \text{ s}^{-1}$) for dirty basal ice below a 210 m thick temperate glacier by means of a three-dimensional simulation. These studies suggest that the large deformation observed in BNU is associated with the presence of liquid water.

Table 2. Calculated Creep Parameters A_4 at 4 m, A_5 at 5 m, and A_{4-5} at 4–5 m Depth as a Function of n Ranging From 1 to 3^a

| Period | $n = 1$ | | | | $n = 2$ | | | | $n = 3$ | | | |
|-----------|--|--|--|-----------|--|--|--|-----------|--|--|--|-----------|
| | A_4 ($10^{-11} \text{ kPa}^{-1} \text{ s}^{-1}$) | A_5 ($10^{-11} \text{ kPa}^{-1} \text{ s}^{-1}$) | A_{4-5} ($10^{-11} \text{ kPa}^{-1} \text{ s}^{-1}$) | H_v (m) | A_4 ($10^{-12} \text{ kPa}^{-2} \text{ s}^{-1}$) | A_5 ($10^{-12} \text{ kPa}^{-2} \text{ s}^{-1}$) | A_{4-5} ($10^{-12} \text{ kPa}^{-2} \text{ s}^{-1}$) | H_v (m) | A_4 ($10^{-14} \text{ kPa}^{-3} \text{ s}^{-1}$) | A_5 ($10^{-14} \text{ kPa}^{-3} \text{ s}^{-1}$) | A_{4-5} ($10^{-14} \text{ kPa}^{-3} \text{ s}^{-1}$) | H_v (m) |
| 2000–2001 | 3.3 | 8.2 | 6.0 | 11.1 | 1.2 | 2.3 | 1.9 | 9.5 | 4.1 | 6.7 | 5.9 | 8.6 |
| 2001–2002 | 1.8 | 4.2 | 3.1 | 12.5 | 0.63 | 1.2 | 0.98 | 10.3 | 2.2 | 3.4 | 3.1 | 9.1 |
| 2002–2003 | 2.4 | 4.8 | 3.7 | 11.9 | 0.86 | 1.4 | 1.2 | 10 | 3.0 | 3.9 | 3.7 | 8.9 |
| 2003–2004 | 2.5 | 6.1 | 4.5 | 11.9 | 0.90 | 1.7 | 1.4 | 9.9 | 3.2 | 5.0 | 4.4 | 8.9 |
| 2004–2005 | 2.3 | 5.5 | 4.0 | 11.3 | 0.81 | 1.6 | 1.3 | 9.6 | 2.9 | 4.5 | 4.0 | 8.6 |

^aThe height of the deformed sediment (H_v) estimated using A_{4-5} is also displayed.

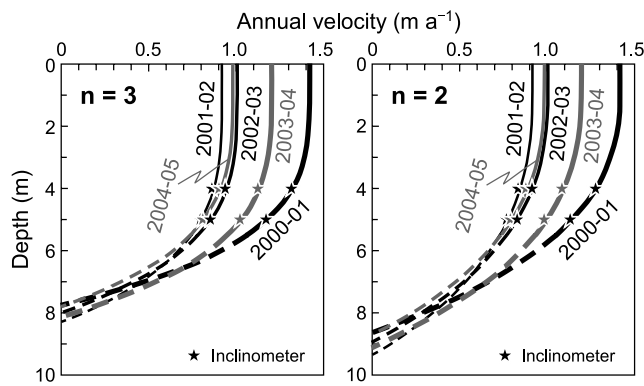


Figure 8. Calculated velocity profiles of BNU. The value n is the exponent of the applied flow law (see text for details).

6.2. Temporal Variation in Deformation

[32] The temporal variations of the movement cannot directly be attributed to the seasonal change in permafrost temperature [cf., *Arenson et al.*, 2002; *Kääb et al.*, 2003], because the strain rates in BNU responded to the ground surface temperatures in spite of the constant temperature ($0.0 \pm 0.2^\circ\text{C}$) at the monitored depths (Figure 6). The constant temperature at the melting point, however, allows liquid water to coexist with ice. The ratio of liquid water to ice possibly changes with seasonal and/or interannual changes in the thermal condition of the active layer. In particular, the rapid increase in the strain rates during the snowmelt period implies that the meltwater infiltrated into the frozen debris (Figure 7), although ice-saturated debris is generally regarded as impermeable [*Andersland et al.*, 1996]. The simultaneous increase in the subzero temperatures in the active layer and the strain rates also indicates that thermal conduction, which possibly affected the temperatures in the permafrost within the resolution of the sensors ($\pm 0.1^\circ\text{C}$), was a minor factor because a timelag originating from thermal conduction should delay the increase in the strain rates.

[33] Two situations are considered for the meltwater infiltration. First, the active layer composed of coarse debris at subzero temperatures easily transports snowmelt water to the frost table, which is indicated by the simultaneous shifts in temperatures to the melting point at different depths (Figure 7) [e.g., *Humlum*, 1997; *Sawada et al.*, 2003]. This is because the coarse materials and steep slope promote drainage in the active layer prior to seasonal frost penetration. Second, the fast deformation of coarse debris filled with ice is probably dilatant, producing a network of air voids that eventually allow water infiltration. This is because the large annual strain rates below 5 m deep ($>0.1 \text{ a}^{-1}$) probably result from thrusting up of debris particles over underlying particles within 1 year. Assuming that A_{4-5} and $n = 2-3$ represent the deformation properties of BNU, the annual strain rates near the frost table (about 2.5 m depth) are calculated to be $0.01-0.03 \text{ a}^{-1}$. The voids produced by such deformation may also result in the water infiltration. In particular, groundwater infiltration from the frost table to the highly deformed layer is most likely to have occurred at

the root (i.e., upper end) of BNU, where the downslope movement of BNU has produced tensile fractures that may penetrate into the perennially frozen layer (Figure 2).

[34] On the assumption of “permeable permafrost,” the annual variation in the strain rates can be explained by the following model (Figure 9):

[35] 1. Air voids have developed in the perennially frozen debris, before the wet front in the snow cover reaches the surface. The larger deformation at a deeper part results in more abundant air voids.

[36] 2. Below the wet snow cover, the weakly frozen active layer is nearly saturated with liquid water. Meltwater infiltration to the perennially frozen debris reduces the effective stress by suddenly increasing the water content, which destabilizes the frozen debris. The increase in the strain rates at both 4 and 5 m depths, often preceding the snow wetting at the ground surface by one to two weeks (Figure 7), indicates that the meltwater originates from somewhere on the upper slope where the snow cover becomes wet earlier than at the monitoring site. The earlier increase in the strain rates at 5 m depth than at 4 m depth (in 2003 and 2005) suggests the presence of different water channels and/or groundwater infiltration from the bottom of the frozen layer.

[37] 3. The water having infiltrated into the active layer and the voids in the perennially frozen layer refreezes and/or drains. As a result, the frozen debris is slightly stabilized.

[38] 4. The strain rates maintained at high values indicate that part of the liquid water remains unfrozen, possibly aided by additional inputs of rainwater and/or meltwater from the thawed active layer.

[39] 5. The strain rates in early winter imply that the pore water at 4 m depth slightly refreezes, while that at 5 m depth remains constant. Slow seasonal freezing under a thick snow cover prevents intensive cooling of the ground and refreezing of the pore water.

[40] 6. Freezing of the active layer leads to refreezing of the pore water, which slows down the deformation, but the continuous deformation in the absence of water infiltration produces a new network of air voids.

[41] This model can also explain the interannual variation in the deformation. In the 2003–2004 period, the deformation from (3) to (5) is larger than the corresponding period in the previous year (Figure 9), which suggests that more abundant air voids are prepared before the following snowmelt season. As a result, infiltration of snowmelt water (7) more effectively destabilizes the frozen debris than in the previous year (2) (Figure 9).

[42] The significant deceleration from 2001 to 2002 and the following slight acceleration during the 2002 snowmelt period (Figure 6) probably resulted from the intensive ground cooling below the thin snow cover in the 2001–2002 winter. The cooling promoted freezing of the pore water from the early winter, which caused the significant deceleration. The resulting poorly developed network of air voids is likely to have prevented meltwater infiltration into the frozen debris. In contrast, the lack of ground cooling below the extremely thick snow cover in the 2000–2001 winter probably prevented freezing of pore water. As a result, the newly developed effective network of air voids may have allowed the water infiltration that resulted in the maximum strain rates in the following snowmelt period.

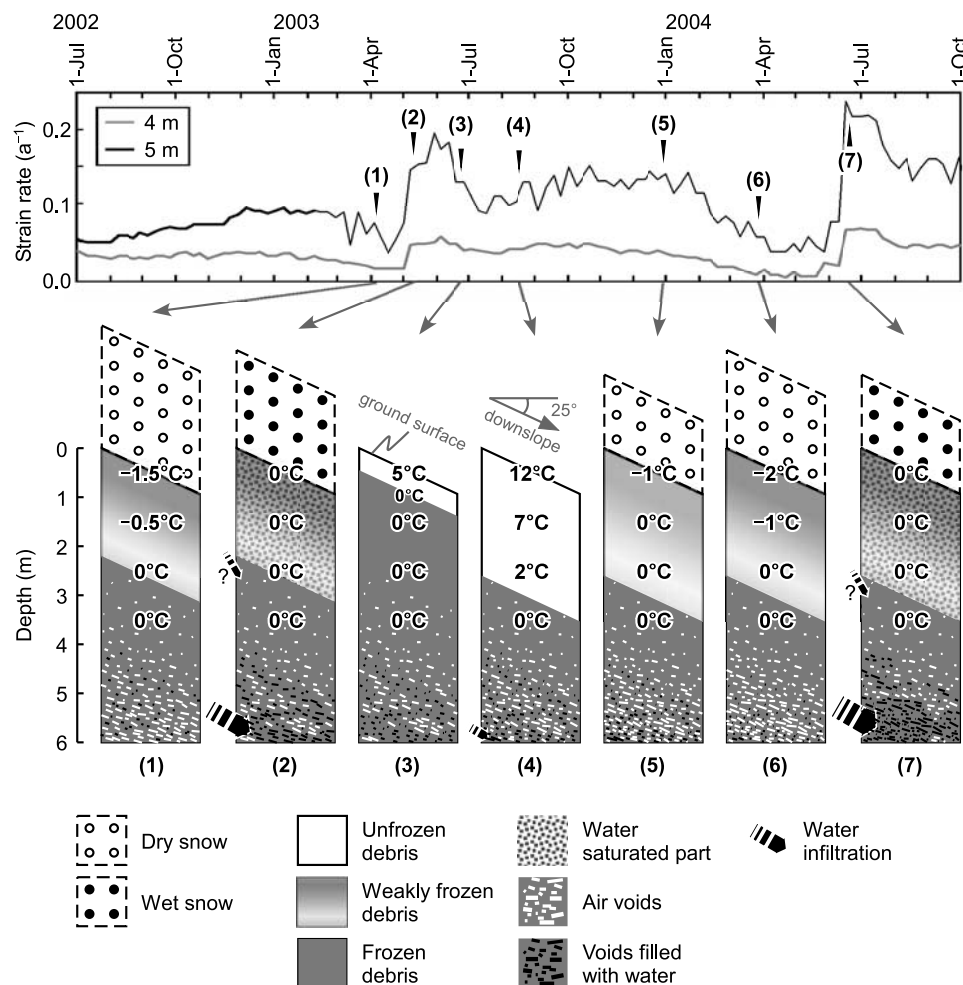


Figure 9. (bottom) Schematic diagram of seasonal and interannual variations of a vertical profile at the monitoring site and (top) strain rates for the modeled duration. The numbers with parentheses correspond to those in the text.

[43] Besides the self-development of air voids, the amount of meltwater and depth of seasonal thawing are also assumed to control the meltwater infiltration. The maximum strain rate in 2001 may have resulted from a large amount of meltwater derived from the unusually thick snow cover. The insufficient water supply from the unusually thin snow cover in 2002 possibly caused the smallest acceleration in the snowmelt period 2002. The extremely hot summer of 2003 promoted lowering of the permafrost table, which may also have resulted in more effective infiltration of meltwater into the underlying frozen layer.

[44] The significant water permeability in a rock glacier was also demonstrated by the recent studies on the boreholes drilled through Murtèl rock glacier, where warm and heterogeneous permafrost occasionally allows liquid water intrusion [Arenson *et al.*, 2002; Vonder Mühll *et al.*, 2003]. This finding of liquid water in the frozen ground supports the idea that liquid water can coexist with ice in some warm rock glaciers. Under such a condition, the amount of liquid water primarily controls the temporal variation in deformation. In fact, similar acceleration in a snowmelt season was also observed on a small rock glacier in the Furgentälti area, Swiss Alps [Mihajlovic *et al.*, 2003]. In addition, the softness of the frozen debris in BNU is most likely to depend on the

liquid water decreasing effective stress in the frozen debris [e.g., Echelmeyer and Wang, 1987; Cohen, 2000].

6.3. Spatial Variations in Deformation

[45] In contrast to the fast movement of BNU, the surface velocities of BNL were small but typical of rock glaciers (Figure 3), although the upper part of BNL had thermal conditions similar to BNU (Figure 4). Ikeda *et al.* [2003] considered that degradation of permafrost inactivated BNL, which was supported by a seismic survey indicating the permafrost table at 4–6 m depth in the lower part of BNL [Ikeda and Matsuoka, 2006]. Thus, thinning of the perennially frozen layer has probably decreased the velocities of the lower BNL. This stable part of the rock glacier dams the downslope deformation of the upper BNL where the permafrost table still lies at 2 m depth. This restriction of downslope movement is also indicated by the uplift component of the velocities on the upper BNL (Table 1).

[46] The warm permafrost of the upper BNL may allow a large A value of the frozen debris, even if the gentle slope and obstacle (i.e., the inactivated lower BNL) result in the relatively small surface velocities. Relatively high DC resistivities, however, indicate a lower liquid water content of the upper BNL compared to that of the BNU [Ikeda *et al.*,

2003]. Thus, the upper BNL probably has an A value smaller than BNU. The deformation of BNL itself is unlikely to be large enough to produce fractures allowing annual water infiltration. Consequently, all of the slope gradient, permafrost thickness, and water content constrain the deformation of BNL.

[47] The velocities of BNL gradually increased from 1998–1999 to 2004–2005 (Table 1). The notable increase from 1999–2000 to 2000–2001 appears to have indirectly been affected by the extremely thick snow cover. Thereafter, the velocities have rarely followed the large interannual variations in ground surface temperatures (Figures 3 and 4). Thus, the perennally frozen debris of BNL was less susceptible to the interannual thermal variations than that of BNU, although its water content is likely to have remained relatively high after the significant supply of snowmelt water in 2000.

[48] Over longer time periods, the large deformation observed on BNU would have led to a pronounced rock glacier landform. However, the short BNU upslope of the relatively long BNL appears to be in the early stage of rock glacier formation. Moreover, the large mass currently transported downslope because of the high speed of BNU is very unlikely to be balanced with the materials supplied from the above [Ikeda et al., 2003]. Both situations suggest that the deformation of BNU is a transient feature. Rising ground temperatures and resulting deformation might have exceeded a certain threshold (e.g., allowing water to infiltrate) at a time before the measurements were started. This might then have accelerated the deformation by some orders of magnitude, which results in the present large difference in the surface velocities between BNU and BNL.

7. Conclusions and Perspectives

[49] Fast deformation of perennally frozen pebbles and cobbles in a layer about 10 m thick was observed during 7 years in a small rock glacier lying at the lower limit of mountain permafrost belt. The frozen debris is more deformable than typical glacier ice at the melting point. The rate of the deformation reflects seasonal and interannual changes in the temperature of the active layer, which is mainly controlled by the thickness and duration of snow cover, whereas the temperature of the frozen debris is almost constant at 0°C. The deformation rate gradually decreases below dry snow cover in winter and rapidly increases during the snowmelt period. These phenomena imply that the frozen debris at the melting point is permeable to snowmelt water.

[50] The large annual strain rates ($>0.1 \text{ a}^{-1}$) of the coarse debris filled with ice probably result from thrusting up of debris particles over underlying particles. The resulting dilatant deformation produces air voids in the frozen debris. In addition, the rapid downslope movement of BNU has produced tensile fractures at the root of the rock glacier. As a result, snowmelt water is likely to infiltrate into the frozen debris through the network of these voids. The infiltrated water seasonally accelerates the permafrost creep by reducing the effective stress, which results in much higher annual velocity than the value expected from the flow law for ice.

[51] The deceleration of the movement between two snowmelt periods is proportional to the cooling intensity in winter, and the acceleration during the early snowmelt

period is proportional to the preceding deformation since the end of the previous snowmelt period. Refreezing of the infiltrated pore water in winter probably decelerates the deformation at the same time as the deformation appears to develop a new network of air voids during this period lacking water infiltration. Thus, larger deformation in a warmer winter more effectively promotes water infiltration in the following snowmelt period. This combination of water infiltration and refreezing is very likely to control the interannual variation in the deformation.

[52] This study suggests that increasing liquid water in perennally frozen debris might have also been responsible for the recent acceleration observed in many rock glaciers in the Alps, where ground temperatures have probably been increasing [Roer et al., 2005; Kääb et al., 2007]. Such slopes located near the lower limit of mountain permafrost might experience rapid acceleration in their deformation in response to atmospheric and ground warming through a positive feedback process: rising temperature leads to increasing deformation, which in turn increases the potential infiltration of water. The latter enhances deformation. This feedback mechanism, which significantly weakens perennally frozen debris, has to be taken into account for climate change impacts on stability of permafrost slopes.

[53] **Acknowledgments.** This study was financially supported by the Grant-in-Aid (15500676 and 17300294) for Scientific Research and Grant-in-Aid for JSPS Fellows from the Ministry of Education, Science, and Culture, Japan and by the Sasakawa Scientific Research Grant from the Japan Scientific Society. The fieldwork by A. Kääb within this study was done at the Department of Geography, University of Zurich, with the help of a number of students from this institution. We also acknowledge F. Keller for logistical help and K. Hirakawa, T. Watanabe, K. Fukui, Y. Sawada, and M. Abe for their cooperation in the field.

References

- Andersland, O. B., D. C. Wiggert, and S. H. Davies (1996), Hydraulic conductivity of frozen granular soils, *J. Environ. Eng.*, **122**, 212–216.
- Arenson, L., M. Hoelzle, and S. Springman (2002), Borehole deformation measurements and internal structures of some rock glaciers in Switzerland, *Permafrost Periglac. Process.*, **13**, 117–135, doi:10.1002/ppp.414.
- Arenson, L. U., and S. M. Springman (2005a), Triaxial constant stress and constant strain rate tests on ice-rich permafrost samples, *Can. Geotech. J.*, **42**, 412–430, doi:10.1139/T04-111.
- Arenson, L. U., and S. M. Springman (2005b), Mathematical descriptions for the behaviour of ice-rich frozen soils at temperatures close to 0°C, *Can. Geotech. J.*, **42**, 431–442, doi:10.1139/T04-109.
- Barsch, D. (1992), Permafrost creep and rockglaciers, *Permafrost Periglac. Process.*, **3**, 175–188.
- Bucki, A. K., and K. A. Echelmeyer (2004), The flow of Fireweed rock glacier, Alaska, USA, *J. Glaciol.*, **50**(168), 76–85.
- Bucki, A. K., K. A. Echelmeyer, and S. MacInnes (2004), The thickness and internal structure of Fireweed rock glacier, Alaska, USA, as determined by geophysical methods, *J. Glaciol.*, **50**(168), 67–75.
- Budd, W. F., and T. H. Jacka (1989), A review of ice rheology for ice sheet modeling, *Cold Reg. Sci. Technol.*, **16**, 107–144.
- Cohen, D. (2000), Rheology of ice at the bed of Engabreen, Norway, *J. Glaciol.*, **46**(155), 611–621.
- Echelmeyer, K., and Z. Wang (1987), Direct observation of basal sliding and deformation of basal drift at subfreezing temperatures, *J. Glaciol.*, **33**(113), 83–98.
- Elconin, R. F., and E. R. LaChapelle (1997), Flow and internal structure of a rock glacier, *J. Glaciol.*, **43**(144), 238–244.
- Frauenfelder, R., and A. Kääb (2000), Towards a paleoclimatic model of rock glacier formation in the Swiss Alps, *Ann. Glaciol.*, **31**, 281–286.
- Frauenfelder, R., W. Haeberli, and M. Hoelzle (2003), Rock glacier occurrence and related terrain parameters in a study area of the Eastern Swiss Alps, in *Permafrost: Proceedings of the 8th International Conference on Permafrost*, edited by M. Phillips, S. M. Springman, and L. U. Arenson, pp. 253–258, A.A. Balkema, Lisse, Netherlands.
- Frauenfelder, R., M. Laustela, and A. Kääb (2005), Relative age dating of Alpine rock glacier surfaces, *Z. Geomorphol.*, **49**, 145–166.

- Glen, J. W. (1955), The creep of polycrystalline ice, *Proc. R. Soc. London Ser. A*, 228, 519–538.
- Gudmundsson, G. H. (1999), A three-dimensional numerical model of the confluence area of Unteraargletscher, Bernese Alps, Switzerland, *J. Glaciol.*, 45(150), 219–230.
- Haeblerli, W. (1985), Creep of mountain permafrost: Internal structure and flow of alpine rock glaciers, in *Mitteilungen der Versuchsanstalt für Wasserbau, Hydrologie und Glaziologie*, vol. 77, 142 pp., Eidg. Tech. Hochsch. Zurich, Zurich, Switzerland.
- Haeblerli, W. (2000), Modern research perspectives relating to permafrost creep and rock glaciers, *Permafrost Periglac. Process.*, 3, 290–293.
- Haeblerli, W., and D. Vonder Mühll (1996), On the characteristics and possible origins of ice in rock glacier permafrost, *Z. Geomorphol. Suppl.*, 104, 43–57.
- Haeblerli, W., L. King, and A. Flotron (1979), Surface movement and lichen-cover studies at the active rock glacier near the Grubengletscher, Wallis, Swiss Alps, *Arct. Alp. Res.*, 11, 421–441.
- Haeblerli, W., A. Kääb, S. Wagner, D. Vonder Mühll, P. Geissler, J. N. Haas, H. Glatzel-Matthäier, and D. Wagenbach (1999), Pollen analysis and ¹⁴C age of moss remains in a permafrost core recovered from the active rock glacier Murtèl-Corvatsch, Swiss Alps: Geomorphological and glaciological implications, *J. Glaciol.*, 45(149), 1–8.
- Haeblerli, W., et al. (2006), Permafrost creep and rock glacier dynamics, *Permafrost Periglac. Process.*, 17, 189–214, doi:10.1002/ppp.561.
- Hoelzle, M., S. Wagner, A. Kääb, and D. Vonder Mühll (1998), Surface movement and internal deformation of ice-rock mixtures within rock glaciers at Pontresina-Schaffberg, Upper Engadin, Switzerland, in *Permafrost: Proceedings of the 7th International Conference on Permafrost*, edited by A. G. Lewkowicz and M. Allard, pp. 465–471, Cent. D'Études Nordiques, Sainte-Foy, Que., Canada.
- Hoelzle, M., M. Wegmann, and B. Krummenacher (1999), Miniature temperature dataloggers for mapping and monitoring of permafrost in high mountain areas: First experience from the Swiss Alps, *Permafrost Periglac. Process.*, 10, 113–124.
- Hoelzle, M., W. Haeblerli, and C. Stocker-Mittaz (2003), Miniature ground temperature data logger measurements 2000–2002 in the Murtèl-Corvatsch area, Eastern Swiss Alps, in *Permafrost: Proceedings of the 8th International Conference on Permafrost*, edited by M. Phillips, S. M. Springman, and L. U. Arenson, pp. 419–424, A.A. Balkema, Lisse, Netherlands.
- Hooke, R. L. (1981), Flow law for polycrystalline ice in glaciers: Comparison of theoretical predictions, laboratory data, and field measurements, *Rev. Geophys.*, 19, 664–672.
- Hooke, R. L., B. B. Dahlin, and M. T. Kauper (1972), Creep of ice containing dispersed fine sand, *J. Glaciol.*, 11(63), 327–346.
- Hubbard, A., H. Blatter, P. Nienow, D. Mair, and B. Hubbard (1998), Comparison of a three-dimensional model for glacier flow with field data from Haut Glacier d'Arolla, Switzerland, *J. Glaciol.*, 44(147), 368–378.
- Humlum, O. (1996), Origin of rock glaciers: Observations from Mellemfjord, Disko Island, central West Greenland, *Permafrost Periglac. Process.*, 7, 361–380.
- Humlum, O. (1997), Active layer thermal regimes at three rock glaciers in Greenland, *Permafrost Periglac. Process.*, 8, 383–408.
- Ikeda, A. (2006), Combination of conventional geophysical methods for sounding the composition of rock glaciers in the Swiss Alps, *Permafrost Periglac. Process.*, 17, 35–48, doi:10.1002/ppp.550.
- Ikeda, A., and N. Matsuoka (2002), Degradation of talus-derived rock glaciers in the Upper Engadin, Swiss Alps, *Permafrost Periglac. Process.*, 13, 145–161, doi:10.1002/ppp.413.
- Ikeda, A., and N. Matsuoka (2006), Pebbly versus bouldery rock glaciers: Morphology, structure and processes, *Geomorphology*, 73, 279–296, doi:10.1016/j.geomorph.2005.07.015.
- Ikeda, A., N. Matsuoka, and A. Kääb (2003), A rapidly moving small rock glacier at the lower limit of the mountain permafrost belt in the Swiss Alps, in *Permafrost: Proceedings of the 8th International Conference on Permafrost*, edited by M. Phillips, S. M. Springman, and L. U. Arenson, pp. 455–460, A.A. Balkema, Lisse, Netherlands.
- Johnson, J. P., Jr., and W. G. Nickling (1979), Englacial temperature and deformation of a rock glacier in the Kluane Range, Yukon Territory, Canada, *Can. J. Earth Sci.*, 16, 2275–2283.
- Kääb, A., and T. Reichmuth (2005), Advance mechanisms of rock glaciers, *Permafrost Periglac. Process.*, 16, 187–193, doi:10.1002/ppp.507.
- Kääb, A., W. Haeblerli, and G. H. Gudmundsson (1997), Analyzing the creep of mountain permafrost using high precision aerial photogrammetry: 25 years of monitoring Gruben rock glacier, Swiss Alps, *Permafrost Periglac. Process.*, 8, 409–426.
- Kääb, A., K. Isaksen, T. Eiken, and H. Farbrot (2002), Geometry and dynamics of two lobe-shaped rock glaciers in the permafrost of Svalbard, *Nor. Geogr. Tidsskr.*, 56, 152–160.
- Kääb, A., V. Kaufmann, R. Ladstädter, and T. Eiken (2003), Rock glacier dynamics: Implications from high-resolution measurements of surface velocity fields, in *Permafrost: Proceedings of the 8th International Conference on Permafrost*, edited by M. Phillips, S. M. Springman, and L. U. Arenson, pp. 501–506, A.A. Balkema, Lisse, Netherlands.
- Kääb, A., R. Frauenfelder, and I. Roer (2007), On the response of rock-glacier creep to surface temperature increase, *Global Planet. Change*, 56, 172–187, doi:10.1016/j.gloplacha.2006.07.005.
- Matsuoka, N. (2001), Solifluction rates, processes and landforms: A global review, *Earth Sci. Rev.*, 55, 107–134.
- Matsuoka, N., K. Hirakawa, T. Watanabe, and K. Moriawaki (1997), Monitoring of periglacial slope processes in the Swiss Alps: The first two years of frost shattering, heave and creep, *Permafrost Periglac. Process.*, 8, 155–177.
- McRoberts, E. C., T. C. Law, and T. K. Murray (1978), Creep tests on undisturbed ice-rich silt, in *Proceedings of the 3rd International Conference on Permafrost*, pp. 539–545, Natl. Res. Council of Can., Ottawa, Ont., Canada.
- Mellor, M., and R. Testa (1969a), Effect of temperature on the creep of ice, *J. Glaciol.*, 8(52), 131–145.
- Mellor, M., and R. Testa (1969b), Creep of ice under low stress, *J. Glaciol.*, 8(52), 147–152.
- Mihajlovic, D., D. Kölbling, I. Kunz, S. Schwab, H. Kienholz, K. Budmiger, M. Imhof, and B. Krummenacher (2003), Developing new methods for monitoring periglacial phenomena, in *Permafrost: Proceedings of the 8th International Conference on Permafrost*, edited by M. Phillips, S. M. Springman, and L. U. Arenson, pp. 765–770, A.A. Balkema, Lisse, Netherlands.
- Morgenstern, N. R., W. D. Roggensack, and J. S. Weaver (1980), The behavior of friction piles in ice and ice-rich soils, *Can. Geotech. J.*, 17, 405–415.
- Nickling, W. G., and L. Bennett (1984), The shear strength characteristics of frozen coarse granular debris, *J. Glaciol.*, 30(106), 348–357.
- Paterson, W. S. B. (1994), *The Physics of Glaciers*, 3rd ed., 481 pp., Elsevier, Oxford, U.K.
- Potter, N., Jr., E. J. Steig, D. H. Clark, M. A. Speece, G. M. Clark, and A. B. Updike (1998), Galena Creek Rock Glacier revisited—New observations on an old controversy, *Geogr. Ann. Ser. A*, 80, 251–265.
- Raymond, C. F. (1980), Temperate valley glaciers, in *Dynamics of Snow and Ice Masses*, edited by S. C. Colbeck, pp. 79–139, Academic, New York.
- Roer, I., A. Kääb, and R. Dikau (2005), Rock glacier acceleration in the Turtmann valley (Swiss Alps): Probable controls, *Nor. Geogr. Tidsskr.*, 59, 157–163, doi:10.1080/00291950510020655.
- Savigny, K. W., and N. R. Morgenstern (1986), Creep behavior of undisturbed clay permafrost, *Can. Geotech. J.*, 23, 515–527.
- Sawada, Y., M. Ishikawa, and Y. Ono (2003), Thermal regime of sporadic permafrost in a block slope on Mt. Nishi-Nupukaushinupri, Hokkaido Island, Northern Japan, *Geomorphology*, 52, 121–130, doi:10.1016/S0169-555X(02)00252-0.
- Strozzi, T., A. Kääb, and R. Frauenfelder (2004), Detecting and quantifying mountain permafrost creep from in situ inventory, space-borne radar interferometry and airborne digital photogrammetry, *Int. J. Remote Sens.*, 25, 2919–2931.
- Vonder Mühll, D., T. Stucki, and W. Haeblerli (1998), Borehole temperatures in Alpine permafrost: A ten years series, in *Permafrost: Proceedings of the 7th International Conference on Permafrost*, edited by A. G. Lewkowicz and M. Allard, pp. 1089–1095.
- Vonder Mühll, D. S., L. U. Arenson, and S. M. Springman (2003), Temperature conditions in two Alpine rock glaciers, in *Permafrost: Proceedings of the 8th International Conference on Permafrost*, edited by M. Phillips, S. M. Springman, and L. U. Arenson, pp. 1195–2000, A.A. Balkema, Lisse, Netherlands.
- Wagner, S. (1992), Creep of alpine permafrost, investigated on the Murtel rock glacier, *Permafrost Periglac. Process.*, 3, 157–162.
- Wahrhaftig, C., and A. Cox (1959), Rock glaciers in the Alaska Range, *Geol. Soc. Am. Bull.*, 70, 383–436.
- Wang, B., and H. M. French (1995), In situ creep of frozen soil, Fenghuo Shan, Tibet Plateau, China, *Can. Geotech. J.*, 32, 545–552.
- Whalley, W. B., and H. E. Martin (1992), Rock glaciers: II models and mechanisms, *Prog. Phys. Geogr.*, 16, 127–186.

A. Ikeda and N. Matsuoka, Graduate School of Life and Environmental Sciences, University of Tsukuba, 1-1-1 Tennodai, Tsukuba, Ibaraki Prefecture, 305-8577 Japan. (aiked@geoenv.tsukuba.ac.jp)

A. Kääb, Department of Geosciences, University of Oslo, P.O. Box 1047 Blindern, N-0316 Oslo, Norway.